

# Origin of Colossal Dielectric Response of $\text{Pr}_{0.6}\text{Ca}_{0.4}\text{MnO}_3$

N. Biškup,\* A. de Andrés, and J.L. Martínez  
*Instituto de Ciencia de Materiales, CSIC, Cantoblanco 28049 Madrid, Spain*

L. Pinsard-Gaudart  
*Laboratoire de Physico-Chimie des Solides 91405 Orsay Cedex - France*  
(Dated: May 23, 2019)

We report the detailed study of dielectric response of  $\text{Pr}_{0.6}\text{Ca}_{0.4}\text{MnO}_3$  (PCMO), member of manganite family showing colossal magnetoresistance. Measurements have been performed on four polycrystalline samples and four single crystals, allowing us to compare and extract the essence of dielectric response in the material. High frequency dielectric function is found to be  $\varepsilon_0=30$ , as expected for the perovskite material. Dielectric relaxation is found in frequency window of 20Hz-1MHz at temperatures of 50-200K that yields to colossal low-frequency dielectric function, i.e. static dielectric constant. Static dielectric constant is always colossal, but varies considerably in different samples from  $\varepsilon_0=10^3$  until  $10^5$ . The measured data can be simulated very well by blocking (surface barrier) capacitance in series with sample resistance. This indicates that the large dielectric constant in PCMO arises from the Schottky barriers at electrical contacts. Measurements in magnetic field and with d.c. bias support this interpretation. Weak anomaly at the charge ordering temperature can also be attributed to interplay of sample and contact resistance. We comment our results in the framework of related studies by other groups.

PACS numbers: 75.47.Lx, 75.47.Gk, 77.22.Ch

## Introduction

The typical value of dielectric constant  $\varepsilon(0)$  in solids is of the order 1-10. Exceptions are ferroelectrics with  $\varepsilon(0) \approx 10^4$  and (charge/spin) density waves materials (CDW/SDW) with  $\varepsilon(0) \approx 10^7$ - $10^9$ . In the former the large dielectric response is a consequence of charge polarization due to ferroelectric displacement of central ion in the unit cell. In the latter, large polarization is achieved by local displacement of electron condensate in density wave. But both of them are unsuitable for applications: ferroelectrics due to limited temperature and frequency range around ferroelectric transition and CDW/SDW materials due to inapplicably low temperatures where density waves occur.

It is therefore understandable that discovery of room temperature frequency independent "colossal" dielectric constant of complex perovskite compound  $\text{CaCu}_3\text{Ti}_4\text{O}_{12}$  (CCTO)<sup>1</sup> sparked the interest in new materials that might not be limited by frequency and temperature. At room temperature CCTO has high dielectric constant ( $\varepsilon(0) \approx 10^4$ - $10^5$ ) that was confirmed in ceramic samples, single crystals and thin films. Theoretical modeling has excluded the possibility of intrinsic origin of high  $\varepsilon(0)$ <sup>2</sup>. These studies conclude that the internal inhomogeneities are in the origin of the effect. It is suspected that those inhomogeneities arise from crystal twinning or some internal domain boundaries. On the other hand, some authors interpret high dielectric response as an artifact coming from Schottky effect at the electrode contacts<sup>3</sup>. In order to solve this dispute, it is useful to study dielectric response in other materials that are known to be inhomogeneous. Manganites are excellent candidates for this purpose.

The family of manganites has attracted a widespread

attention of scientific community in the last 15 years due to their "colossal" magnetoresistance<sup>4</sup>. The magnetoresistive effects in some compositions reach the factor of  $10^6$ , which essentially means magnetic field induced insulator-metal transitions. In order to understand such colossal effects, the concept of phase separation has emerged. The ground state of certain manganite compounds<sup>5,6</sup> is proved to be inhomogeneous, consisting typically of metallic clusters in an insulating/semiconducting matrix. Such a separation of phases (metallic and insulating) is believed to be the cause of many unusual phenomena, including colossal magnetoresistance. The purpose of this work is to investigate if the phase separating boundaries can contribute to the dielectric response.

The general formula for manganites is  $\text{R}_{1-x}\text{A}_x\text{MnO}_3$  where R stands for rare earth (La, Pr) and A for any divalent atom (Ca, Sr). Among various manganites,  $\text{Pr}_{1-x}\text{Ca}_x\text{MnO}_3$  is unique, showing insulating behaviour over the whole composition (x) range due to its narrow bandwidth of 3d conducting  $e_g$  electrons<sup>7</sup>. The title compound  $\text{Pr}_{0.6}\text{Ca}_{0.4}\text{MnO}_3$  falls in the range  $0.3 < x < 0.75$  where the ground state is charge ordered antiferromagnetic insulator<sup>8,9</sup>. Charge ordering refers to ordering of manganese ions that can be in  $\text{Mn}^{3+}$  or  $\text{Mn}^{4+}$  valence: at low temperatures these ions order into a superstructure forming stripes of  $\text{Mn}^{3+}$  and  $\text{Mn}^{4+}$  ions. Magnetization measurements in the title compound show two transition at  $T=240$  and  $T=180\text{K}$  that are believed to be charge ( $T_{CO}$ ) and antiferromagnetic ordering ( $T_{AF}$ ), respectively. Insulator-metal transition in title compound can be induced by magnetic field<sup>7</sup>, electric current<sup>10</sup>, pressure<sup>11</sup> or X-rays<sup>12</sup>. These and other studies<sup>13,14,15</sup> converged around the idea of phase separation involv-

ing ferromagnetic metallic droplets coalescing and enabling the current percolation through the insulating matrix. The origin of phase separation lies in existence of structural inhomogeneities (clusters) associated with charge ordering<sup>16,17</sup>. Recent report of nanoscale competition in charge ordered LCMO<sup>18</sup> indicates that even the same phases (charge ordered insulator) form clusters with different orientation of CO stripes. The formation of clusters generally precedes structural or magnetic transitions<sup>19</sup> arising at temperature  $T^* > T_C$  (in our case  $T_C = T_{CO}$ ). PCMO system is thus ideal to study dielectric response of the inhomogeneous (clustered) system. Several groups already reported colossal dielectric response in magnetoresistive materials and recently it is also reported in  $Pr_{0.67}Ca_{0.33}MnO_3$  ( $x=1/3$ )<sup>20</sup>. In the latter case it is suggested that it arises from CDW orderings or phase separation inhomogeneities. We have performed detailed study on similar system (PCMO with  $x=3/8$ ) in order to resolve the origin of apparent colossal dielectric response in PCMO.

After this introduction, we give an overview of experimental methods. In results we report on four topics: resistive characterization, dielectric response in temperature, influence of magnetic field and influence of d.c. bias. Discussion is following each of these measurement reports. In Summary we bring the conclusions and comment our findings in the light of related reports.

## Experimental

We have measured 4 polycrystalline (PC) samples (P1-P4) and 4 single crystals (SC, S1-S4) which enables us to extract the data inherent to the material itself and test and compare the findings. Single crystal samples are plates that are cut from the single rod which long axis coincide with crystal (001) direction (inside 15 degrees). Single crystal measurements for samples S1-S3 are with current contacts in this (001) direction while contacts for S4 are in perpendicular direction. The nominal composition of polycrystals ( $Pr_{0.6}Ca_{0.4}MnO_3$ ) differs slightly from the single crystals ( $Pr_{0.625}Ca_{0.375}MnO_3$ ) but their characterization shows almost identical behaviour (Figure 1). Samples are first characterized magnetically (SQUID), later electrically (four-contact configuration) and then prepared for the capacitance measurements (two-contact configuration). Care was taken to reduce the parasite capacitances of measurement system below 3pF in order to have measurable signal even in the high frequency limit ( $\epsilon_{HF}$ ). Dielectric measurements are done with Quadtech LCR-meter, model 1920. The voltage applied was always at low limit of 20mV in order to minimize the effects of voltage-current nonlinearity. The frequency range covered by this instrument lies between 20Hz and 1MHz. At low temperatures the relaxation times for colossal dielectric response drop below our frequency window. Here we measured dielectric constant/capacitance through the time dependent charging effect by sourcemeter Keithley 2410.

## Results and discussion

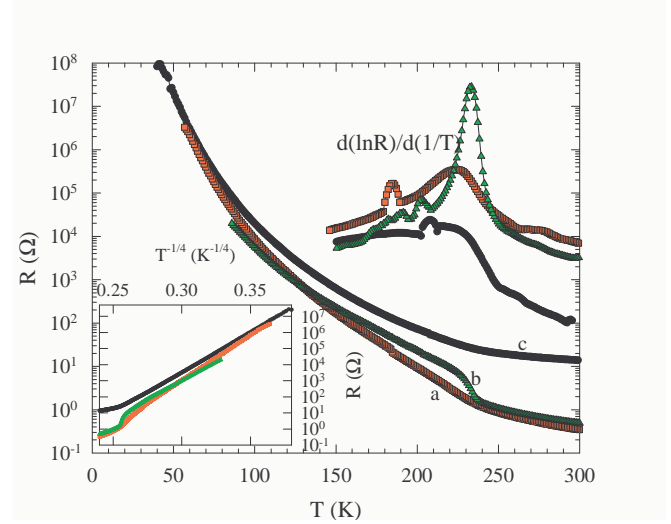


FIG. 1: (Color online) Temperature dependent resistance of polycrystal P1  $Pr_{0.6}Ca_{0.4}MnO_3$  (a, squares) and single crystal S1  $Pr_{5/8}Ca_{3/8}MnO_3$  (b, triangles). Circles (c) stand for two contact (capacitance) configuration of P1 sample. In the right inset is  $d(\ln R)/d(1/T)$  indicating  $T_{CO}$ . In the left inset is resistance over  $T^{-1/4}$  indicating three dimensional variable range hopping.

### Resistive characterization

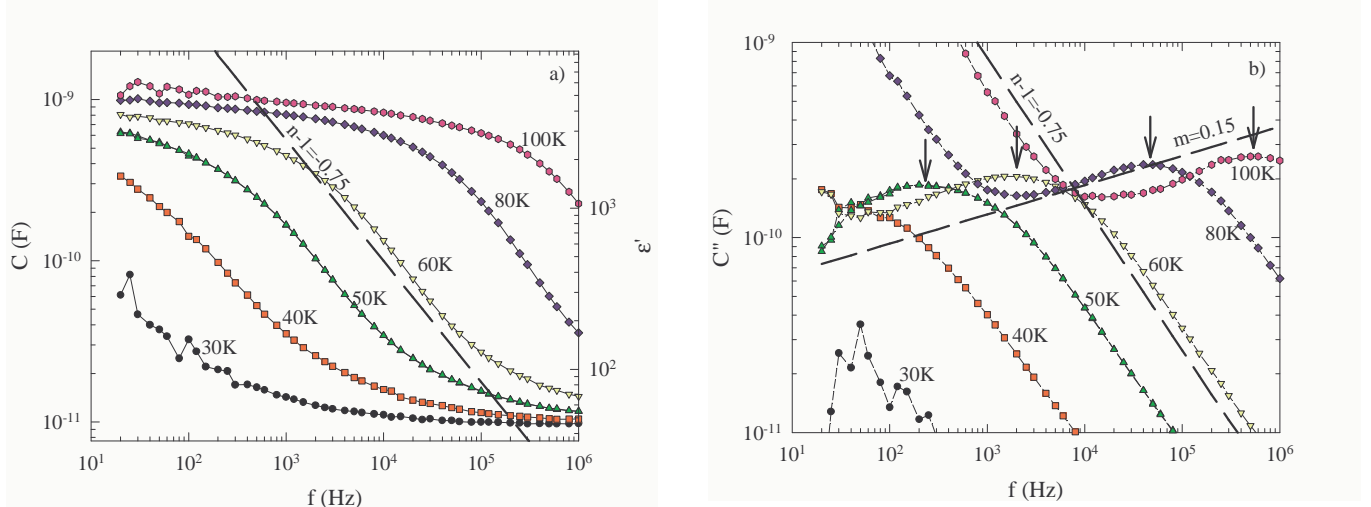
Figure 1 shows the resistive characterization of representative polycrystalline (P1) and single crystal (S1) samples. The charge ordering transition, interpreted as the peak in the derivative  $d(\ln R)/d(1/T)$ , appears at  $T_{CO}=225$  and  $235$ K, respectively. These values are very close, especially in the light of "broad" peak in polycrystalline sample. Magnetization data give identical value for both cases of  $T_{CO}=235$ K. The antiferromagnetic ordering at  $175$ K is detectable only in the magnetization measurements. The insulating behaviour below  $T_{CO}$  is governed by three-dimensional ( $d=3$ ) variable range hopping<sup>21</sup> where electrical conductivity follows

$$\sigma_{DC} = \sigma_0 e^{-(\frac{T_0}{T})^{\frac{1}{1+d}}} \quad (1)$$

with  $T_0=3.2$ K. Further, all data from resistive measurements (resistivity in polycrystal and two perpendicular directions in single crystals, as well as measurements in magnetic field) show no sign of anisotropy. This enables us to treat identically the dielectric response in polycrystalline and single crystal samples. From Figure 1 we can also estimate the influence of contact resistances in two-probe measurements, which, as expected, becomes negligible at low temperatures.

### Dielectric response and its temperature dependence

The most instructive presentation of dielectric data is given in the terms of frequency dependent dielectric permittivity/capacitance<sup>22</sup> - the method that is followed here. Dielectric data are collected measuring real ( $G$ )



and imaginary (B) part of electrical admittance. The dielectric permittivity  $\varepsilon$  is related to electrical conductivity  $\sigma$  as:

$$\varepsilon'(\omega) = \frac{1}{\varepsilon_0} \frac{\sigma''(\omega)}{\omega} = \frac{1}{\varepsilon_0} \frac{B(\omega) \frac{l}{s}}{\omega} \quad (2a)$$

$$\varepsilon''(\omega) = \frac{1}{\varepsilon_0} \frac{\sigma'(\omega) - \sigma_{DC}}{\omega} = \frac{1}{\varepsilon_0} \frac{[G(\omega) - G_{DC}] \frac{l}{s}}{\omega} \quad (2b)$$

where  $l$  and  $s$  stand for thickness and cross section of the sample, respectively.  $\varepsilon_0$  is permittivity of vacuum:  $\varepsilon_0 = 8.85 \times 10^{-12}$  F/m. As can be seen from eq. 2b, the d.c. conductance does not contribute to the dielectric response since these two are, for the most part, independent processes<sup>22</sup>. Capacitance is directly related to dielectric constant as  $C = \varepsilon_0 \varepsilon (s/l)$  and in this report we present data in this form. Figures 2 shows the typical frequency response of PCMO system: Fig 2a shows real part of dielectric function and 2b imaginary part. The data in figures 2 correspond to P1 polycrystal but represent very well the response of all eight samples. For the clearness of the data, we present dielectric relaxation in log-log plot that reveals relaxation exponents (see below) although the loss peak in log-log presentation is not so pronounced like in semi-log plot, especially due to "leaking condenser" tail. Dielectric relaxation in this sample is observed for temperatures lower than 100K when real part of dielectric function  $\varepsilon'$  decreases with increasing frequency. At the same time, as a consequence of Kramers-Kronig rule, the imaginary part of dielectric function shows "loss peak" that is indicated with arrows in Fig. 2b. This low-frequency relaxation (where "low" stands for frequencies much smaller than plasma frequency  $\omega_P = 10^{10}$ - $10^{12}$  Hz) is very reminiscent to the popular Debye relaxation, having well defined 'loss peak' in  $\varepsilon''$ . Phenomenologically, such relaxation is given by:

$$\varepsilon(\omega) = \varepsilon_{HF} + [\varepsilon(0) - \varepsilon_{HF}] \frac{1}{1 - i\omega\tau_0} \quad (3)$$

FIG. 2: (Color online) Dielectric relaxation for polycrystal P1 at temperatures given in the figures. Dashed lines indicate slopes defined in text. a)  $C'(\omega)$ . On the right scale is value of dielectric function. b)  $C''(\omega)$ . Arrows denote loss peaks.

where  $\tau_0$  denotes characteristic low-frequency relaxation time  $\tau_0 = 1/\omega_0$ .  $\varepsilon(0)$  is dielectric constant and  $\varepsilon_{HF}$  stands for high frequency dielectric function, i.e. at  $\omega \gg \omega_0 = 1/\tau_0$ . In the limit  $\varepsilon_{HF} \rightarrow 0$  this expression corresponds to 'Debye' equivalent circuit consisting of resistance  $R$  coupled serially to capacitance  $C$  as shown in Figure 4a<sup>22</sup>. Relaxation time  $\tau_0$  in such equivalent circuit is given by  $\tau_0 = RC$  and at frequencies above relaxation ( $\omega > \omega_0 = 1/\tau_0$ , real and imaginary part of complex 'capacitance' follow  $\omega^{-2}$  and  $\omega^{-1}$  dependence, respectively. Note however that corresponding exponents in Fig. 2 are lower than in this ideal (Debye) case, as it could be expected for a real material.

Debye theory was developed in 1912 for dielectric response of floating dipoles in viscous (liquid) medium. It is therefore clear that this theory isn't adequate description of dielectric phenomena in solids. Its popularity in solid state physics community is based on the fact that many solids exhibit similar behaviour to Debye's model, thinking primarily on low-frequency ( $\omega_0 \ll \omega_P$ ) relaxation and according loss peak. The correct treatment of dielectrics in solid state is expected from many-body theory that treats the screening of outer electric field by quasiparticle excitations in solids. Disado and Hill<sup>23</sup> have developed universal model for dielectric relaxation that is able to explain the whole range of dielectric relaxation with or without loss peak. Moreover, their theory explains the absence of logarithmic relaxation in solids and universality of power-law relaxations. Namely, the vast amount of empirical data on the dielectric relaxation in solids shows that all of them can be represented by universal power-law ( $\varepsilon \propto \omega^m$  and  $\varepsilon \propto \omega^{n-1}$ ) involving exponents  $m$  and  $n$  coming through the tunneling transitions between two preferred dipolar configuration. These transitions are not linked to the phonon bath and are therefore tempera-

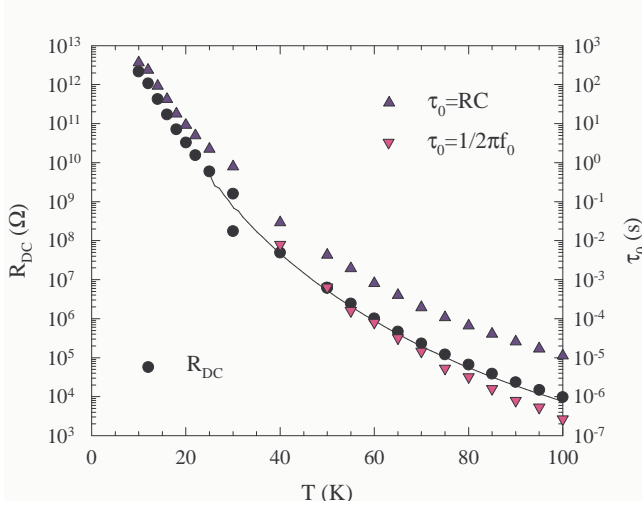


FIG. 3: (Color online) Fig. 3 Relaxation time  $\tau_0$  as a function of temperature (right axis). See text for point assignment. On the left axis is samples resistance (circles and line).

ture independent. Such exponents (low-frequency slope  $m$  and high-frequency slope  $n-1$ ) are drawn as guide to the eye in Figure 2b. Power law relaxation is successfully explaining discrepancy from such exponents in ideal Debye case without introduction of additional phenomenological parameters. 'Debye' loss peak in solids is then appearing through so-called "large transitions" between two dipolar orientations that are separated by potential barrier and are thermally assisted. From this thermal assistance it is clear that temperature behaviour of the loss-peak frequency in solids has to follow the same behaviour as charges involved in electrical transport, i.e. as samples resistance. This can be seen as well in Fig. 3. Here the resistance  $R$  of sample P1 (left axis) is plotted together with 'Debye' relaxation time  $\tau_0=1/\omega_0$  (right axis) for temperatures below 100K. All data are from two contact measurements: line and solid circles denote  $R_{DC}$  data taken by electrometer and LCR-meter, respectively. At  $T \leq 30$ K relaxation falls below our frequency window. At these temperatures capacitance  $C$  and resistance  $R$  are measured through time dependence of charging process. Voltage at the electrodes is built up according to  $V(t)=V_0(1-e^{-\frac{t}{RC}})$ , which extends our temperature range for capacitance measurements down to  $T=10$ K. Triangles pointing up are simply product of resistance and capacitance  $\tau_0=RC$ , while those pointing down are taken from the loss peak frequency  $\tau_0=1/2\pi f_0$ , as indicated in figure 2b. The discrepancy of two "definitions" of  $\tau_0$  decreases with decreasing temperature and tends to diminish at very low temperatures where contact resistance becomes negligible comparing to intrinsic sample resistance entering into  $\tau_0=RC$ . This will be an important argument in considerations below.

As we can see from figures 2 and 3, our dielectric data can be represented quite well by Debye equivalent circuit as in Fig. 4a. Smaller relaxation exponents ( $n$  and

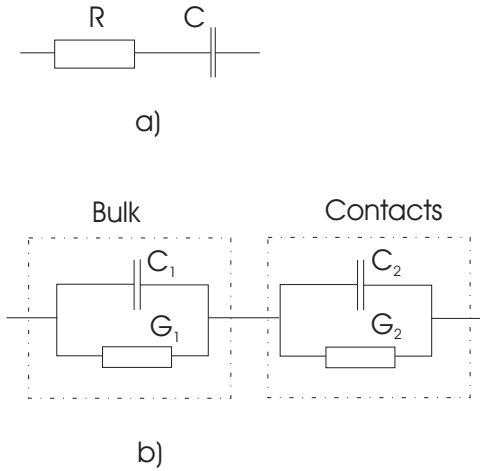


FIG. 4: Equivalent circuits for: a) ideal Debye response b) combination of bulk and surface components.

m) in sample P1 shouldn't be surprising since equivalent circuits consist of ideal elements (capacitances and resistances) while in real material we might have non-ideal/leaking capacitances and resistances. High frequency capacitance, when parasite capacitance is subtracted, gives  $\epsilon_{HF}=30$ , as expected for perovskites. Low frequency capacitance of sample P1 gives colossal values of  $\epsilon(0) \simeq 5000$ . In order to verify these data, we have measured four polycrystalline samples and four single crystals and, although varying considerably, dielectric constant always shows "colossal" values above  $10^3$ . Dielectric constant and relevant data for all 8 samples are presented in Table 1. Value of dielectric constant is deduced

sample	area (mm <sup>2</sup> )	thickness (mm)	contact type	$R_{RT}$ ( $\Omega$ )	$C(0)$ (nF)	$\epsilon(0)$	
P1	12	0.5	Agpaint	10	1	$5 \cdot 10^3$	
P2	13.2	1.2	filmAu	9	2	$2 \cdot 10^4$	
P3	7	1.2	filmAu	24	10	$1.9 \cdot 10^5$	
P4	4.1	0.63	Agpaint	20	0.12	$3 \cdot 10^3$	
S1	9	0.25	Agpaint	2	0.4	$1.3 \cdot 10^3$	
S2	9	0.65	Agpaint	3	0.25	$2 \cdot 10^3$	
S3	7.2	0.58	Agpaint	54	0.14	$1.3 \cdot 10^3$	
				filmAu	35	5	$4.5 \cdot 10^4$
S4	2.9	1.4	filmAu	98	2	$1.1 \cdot 10^5$	

TABLE I: Some relevant parameters of eight samples in this study. All resistances are from two-contact measurements

by extrapolation of flat part of  $\epsilon'$  (i.e. at  $\omega \ll \omega_0$ ) toward zero frequency. One can see that lowest dielectric constant (and capacitance) have samples with contacts made directly with silver paint. Samples with preevaporated gold contacts show much higher dielectric constant:  $\epsilon(0) \geq 10^4$  despite higher (or just because of it!) contact resistances. It can be also seen that capacitance doesn't depend (at least significantly) on geometrical factors. All

of the above suggest that dielectric response in PCMO is governed by contacts. Let's see if we can model our dielectric response with different equivalent circuit.

Figure 4b shows a typical circuit that represents both bulk and surface (blocking) capacitances. Both of them are parallel accompanied by their corresponding resistances or, as noted in the Figure 4b, by conductances  $G_i=1/R_i$ . Solving complex conductivity for such circuit enables us to calculate the frequency response. Zero frequency capacitance  $C(0)$  is given by:

$$C(0) = \frac{G_1^2 C_2 + G_2^2 C_1}{(G_1 + G_2)^2} \quad (4)$$

In the high temperature limit we assume  $G_2 \ll G_1$  that yields to  $C(0) = C_2$  and in low temperature limit  $G_2 \gg G_1$  yielding  $C(0) = C_1$ . Between these two limits we have complex interplay of conductances  $G_1$  and  $G_2$  that determines capacitance  $C(0)$  and relaxation time  $\tau_0$ . Let's now assume that bulk capacitance  $C_1$  equals to high frequency limit of capacitance in Fig. 2, i.e.  $C_1 = 10\text{pF}$ . Surface or contact capacitance is then the one of low frequency limit, i.e.  $C_2 = 1\text{nF}$ . Let's estimate the values of  $G$ 's for sample P1 from figure 1. Let us consider that four contact measurements give bulk resistance (conductance) without contact resistances. The difference between two and four contacts then gives the resistance of contacts  $1/G_2 = R_{\text{cont}} = (R_{2\text{cont}} - R_{4\text{cont}})$ . (This is just an estimate since contacts on the sample, as well as effective geometrical factors, are distinct in the case of 2-contact and 4-contact measurements). Figure 5 shows frequency dependent capacitance for such a simulation for set of temperatures. One can see that our rough estimate simulates quite well real data from Figure 2. According to Fig. 4a, apparent decrease of capacitance  $C(0)$  at low temperatures in Fig. 2a could be interpreted just by inherent decrease of capacitance  $C$ . Contrary to this, in Figs. 4b and 5 we assume constant capacitances  $C_1$  and  $C_2$  and the decrease of measured capacitance  $C$  is associated to diminishing contribution of contacts in overall resistance (decreasing  $R_2/R_1 = G_1/G_2$ ). Relaxation time  $\tau_0$  is in the low temperature limit ( $G_2 > G_1$ ) given predominantly by  $G_1$ , like in the typical Debye case ( $R_1 = 1/G_1$  in series with  $C_2$ ). Note further that two definitions of  $\tau_0$  plotted in Fig. 3 differ more at high temperatures and converge toward low temperatures. This convergence illustrates diminishing contribution of contact resistance  $R_2$  in  $R = R_1 + R_2$  since real relaxation time  $\tau_0$  (measured by dielectric relaxation) is defined by bulk resistance  $\tau_0 = R_1 C_2$  and not by overall resistance  $R = R_1 + R_2$ . Our low-frequency relaxation thus seems to come from contact capacitances.

In Table 1 we have listed values of capacitances  $C(0)$  for our eight samples. These are the values at room temperature (RT) that are either measured directly or deduced from the low temperature measurements. Namely, due to small resistance of PCMO samples at room temperatures, dielectric measurements are impeded by both

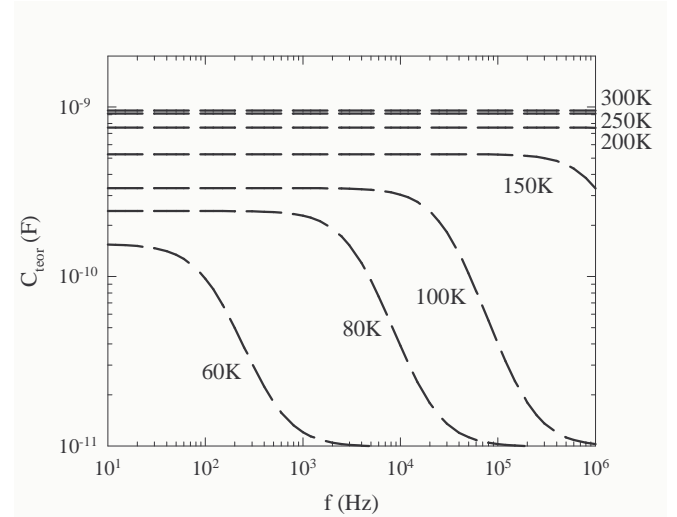


FIG. 5: Simulation of capacitance of circuit in diagram 4b using values from Fig. 2. See text.

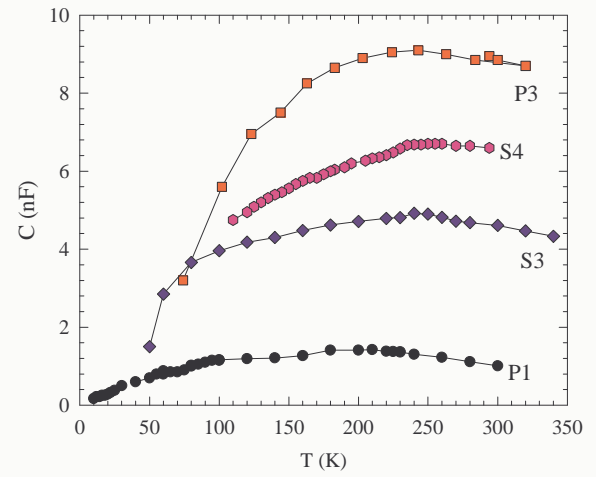


FIG. 6: (Color online) Temperature dependence of capacitance  $C(0)$  for four different samples.

inductances and sensitivity of measuring instrument, especially at low frequencies. Thus, we were able to record RT capacitances directly only in samples with high  $C(0)$ . Figure 6 presents  $C(0)$  values for four of our samples up to (and above) room temperature. One can see once again that the capacitance increases with temperature and becomes nearly temperature independent toward RT. This justifies our estimate of RT capacitances of other four samples. However, Figure 6 reveals a weak anomaly at temperatures close to  $T_{CO}$ . The model from Fig. 4 can't explain the decrease of  $C(0)$  at  $T > T_{CO}$ . It appears that dielectric response in PCMO is influenced by bulk properties, indeed. Let's probe it by other methods.

#### Measurements in magnetic field

The influence of magnetic field on dielectric response

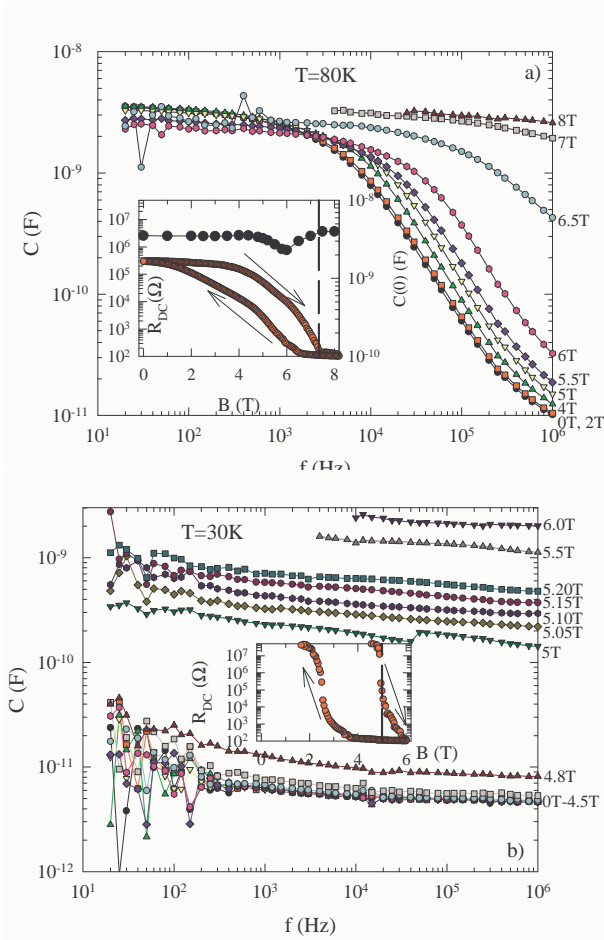


FIG. 7: (Color online) Effect of magnetic field on capacitance at a)  $T=80\text{K}$  and b)  $T=30\text{K}$  for sample S3. Values of magnetic field are given on the right axis. Insets show d.c. resistance as a function of field. Broken lines indicate ferromagnetic transition  $B_m$  as deduced from up-field magnetization measurements. Solid circles in inset of 7a denote capacitance  $C(0)$ .

in PCMO is clearly one of the most intriguing questions, having in mind colossal effects of magnetic field on materials resistance. Figures 7a and 7b present the influence of magnetic field on the real part of dielectric function  $\epsilon$  for  $T=80\text{K}$  and  $T=30\text{K}$ , respectively, for single crystal sample S3. Insets present d.c. resistance curves in field. These insets are excellent examples of colossal magnetoresistance effect. At field strengths above several tesla, the resistance drops for several orders of magnitude. This is the consequence of magnetic field induced ferromagnetic transition<sup>24</sup>. Our magnetization measurements, as well as hysteresis in resistive measurements, show that these transitions are of first order. At  $T=80\text{K}$ , the resistance decreases rather smoothly in magnetic field until first order transition field of  $B_m=7.35\text{T}$  (as deduced by magnetization measurements) that is indicated by vertical line. At  $B=0\text{T}$  resistance is already low enough and we observe relaxation in our frequency window. In this

resistance range  $\tau_0$  is given mainly by  $R_1=1/G_1$  and decrease of resistance enables us to follow adjacent decrease of relaxation time  $\tau_0$ . At the same time, capacitance remains roughly constant. From the data presented in Fig. 7a we see that this case resembles very closely the ordinary, zero-field temperature dependence (Fig. 2). Note also that the relaxation observed in 80K case is at fields lower than  $B_m$ .

Situation is different at  $T=30\text{K}$ . At 30K and zero magnetic field dielectric relaxation falls below our frequency window ( $f_0 < 20\text{Hz}$ ). Therefore, what we see at this field is high frequency tail of our relaxation giving high-frequency dielectric function  $\epsilon_{HF} \approx 30$ . However, with increasing field, i.e. decreasing resistance, one would expect to see low-frequency relaxation reappearing as in Fig. 2a. Instead, dielectric response increases abruptly, keeping its frequency independent (flat) shape to the highest fields. It is difficult to explain a raise of capacitance at constant temperature for different fields/resistances if one would assume single element (bulk) source. But if one assumes double capacitances like in Fig. 4b, one can simulate this increase. Modeling resistances from eq. 4 approximately yield to  $C(0) \propto R_2/R_1$ . Raise of capacitance thus suggests that contact resistance  $R_2$  doesn't decrease with field as fast as bulk resistance  $R_1$ . This shouldn't be unexpected if one recalls that contact region should be the region with larger imperfections. Since the bulk insulator-metal transition is connected with ferromagnetic ordering, it is expectable that ferromagnetic ordering (i.e smaller resistance) is impeded at sample boundaries, close to electrodes. Such an interpretation is in accordance with rather high resistance ( $R=R_1+R_2=100\Omega$ ) above  $B_m$  - this resistance is presumably coming from contacts. In this way interplay of resistances  $R_1=1/G_1$  and  $R_2=1/G_2$  give the same increase of  $C(0)$  like in Figures 2a and 5. The fact that 30K case lacks the relaxation that would be expected from gradual increase of  $R_1$  (capacitance in Fig. 7b is nearly flat in frequency), can be explained by correlation effects in ferromagnetic phase. Dielectric response of systems with strong correlation is rigid, i.e. it doesn't relax<sup>22</sup>. This is exhibited by flattening/disappearance of the loss peak and corresponding effect in its real counterpart. Contrary to this, at  $T=80\text{K}$  we observe the relaxation since these measurements are done in antiferromagnetic phase ( $B < B_m$ ), equally as measurements without magnetic field. Bulk and contact resistance here depend similarly on magnetic field (see figure 1) and  $C(0) \propto R_2/R_1$  remains approximately constant. Small twist of  $C(0)$  around  $B=6\text{T}$  can be associated exactly with the change in resistance ratio  $R_2/R_1$  close to ferromagnetic transition.

#### Measurements with d.c. bias

As already mentioned in introduction, the PCMO system is susceptible to applied electric field, the effect that for high voltages leads to insulator-metal transition. But even below this threshold field, the current-voltage characteristic is nonlinear showing decrease of resistance with

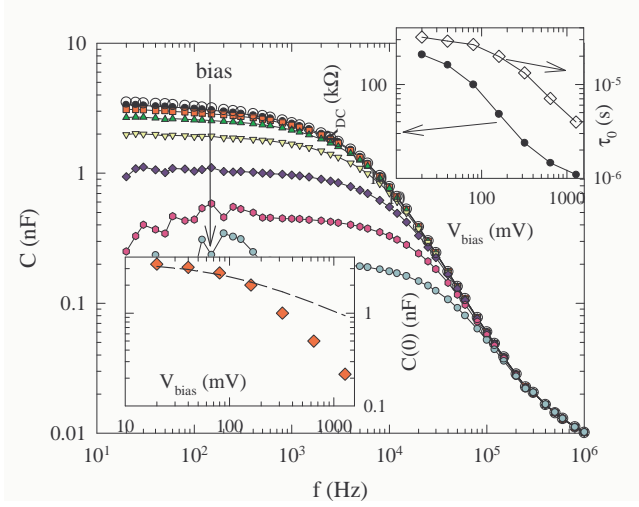


FIG. 8: (Color online) Effect of d.c. bias on capacitance at  $T=80\text{K}$  for sample S3. Arrow indicates increasing bias voltage - voltages are as shown in the inset. Right inset: resistance  $R_{DC}$  (circles, left axis) and relaxation time  $\tau_0$  (diamonds, right axis) as a function of d.c. bias voltage. Left inset: capacitance  $C(0)$  (diamonds) vs. bias voltage. Broken line is an estimate according to eq. 5.

increase of voltage. This nonlinearity can't be explained solely by heating effects since at temperatures below 60K it is observed even for heating power less than 1pW. It is therefore interesting to see the effect of voltage on dielectric response. We have performed dielectric measurements for a set of a.c. excitation voltages and also those biased by d.c. voltage. They are essentially identical so we present here just d.c. biased measurements. Figure 8 shows such measurements for single crystal S3 at  $T=80\text{K}$ . Capacitance is shown for a set of d.c. bias voltages ( $V_{bias}=0, 20, 40, 80, 160, 320, 640$  and  $1280\text{mV}$ ). The a.c. excitation was always kept at the lowest level of  $V=20\text{mV}$ . In the upper right inset is the effect of bias on sample resistance (circles - left axis) and relaxation time  $\tau_0$  (diamonds - right axis). Resistance decreases for more than one order of magnitude for this range of voltages. Its origin is clearly not heating since resistance at this temperature decreases even for heating power of 10nW. As in all previous (zero-bias) cases in this study, the relaxation time  $\tau_0$  follows the resistance, i.e. decreasing resistance is accompanied by decreasing  $\tau_0$ . However, we can see that this correspondence is not perfect:  $\tau_0$  decreases nine times while resistance drops twenty-two times. If we recall our model in Fig.4b, and remember that  $\tau_0 \propto R_1$ , this means that contact resistance  $R_2$  coming from our measured resistance  $R$  ( $R=R_1+R_2$ ) is responsible for stronger decrease of  $R$  than expected from  $\tau_0 \propto R_1$ . But the most important feature here is the decrease of capacitance with bias voltage (and decreasing resistance). This effect is opposite than observed at temperature dependence of non-biased measurements (see for example Fig. 6).

It is well known that metal-semiconductor contact usually results in Schottky barrier. A region of semiconductor in direct contact with metal is depleted of carriers as a consequence of different band levels in both materials. This depletion layer thus depends on type of metal, i.e. its energy band. The width  $w$  of depletion layer is given by

$$w = \sqrt{\frac{2\epsilon}{qN_D}(V_b - V_a)} \quad (5)$$

where  $V_b$  stands for internal, junction voltage and  $V_a$  for external, applied voltage.  $\epsilon$  is dielectric constant of semiconductor,  $q$  electron charge and  $N_D$  impurity concentration. Schottky contacts always present a capacitance  $C=\epsilon S/w$  that, as seen from eq. 5, depends as  $C \propto w^{-1} \propto (V_b - V_a)^{-1/2}$ . In ideal Schottky semiconductor case (one contact perfectly ohmic and another with Schottky barrier) applied voltage  $V_a$  is supposed to be in reverse direction (negative) in order to decrease capacitance. In our case that has two equivalent Schottky contacts, situation becomes more complicated. But overall behaviour is the same. In the left inset we plot  $C(0)$  vs.  $V_{bias}$  as deducted from Fig.8. We also plot a line that fits to calculated data and is calculated by eq. 5 using  $V_b=0.1\text{V}$ , as estimated roughly from  $R(T)$  measurement. This estimate fits quite well to measured data for small voltages, i.e. for voltages smaller than Schottky breakthrough voltage. The decrease of capacitance with voltage can be therefore interpreted by Schottky effect. And finally, current-voltage nonlinearity (shown in our case as decreasing resistance with applied voltage) is the basic property of Schottky diodes. It thus becomes evident that dielectric response in PCMO, as well as related nonlinear effects, has the origin in Schottky barriers at metallic contacts. This also explains dependence of capacitances on type of contacts (Au film or Ag paint).

### Summary

We have performed detailed analysis of "colossal" dielectric response in  $\text{Pr}_{0.6}\text{Ca}_{0.4}\text{MnO}_3$ . Dielectric relaxation and decrease of capacitance at low temperatures are associated with the interplay of surface and bulk capacitances and their related resistances. Change of capacitance with magnetic field can be equally well explained by surface (contact) capacitances. Dependence of dielectric response on voltage (both d.c. and a.c.) can be explained only as a consequence of Schottky layers in contact with electrodes. This interpretation is in accordance with dependence of capacitance on metal used as the electrode. All of the above suggest that bulk properties of title material are not responsible for dielectric response: dielectric constant of title material is  $\epsilon(0)=\epsilon_{HF}=30$ , as expected for perovskites. None of the intriguing physical properties of PCMO (charge ordering, antiferro and ferromagnetism, clusters) seem to influence dielectric response. The only feature resembling to bulk property of PCMO is a weak anomaly at temperatures close to temperature of charge ordering. Decrease of capacitance with

temperature for  $T > T_{CO}$  can't be explained in the frame of diagram in Fig. 4b. However, it might be evident that contact (Schottky) capacitance  $C_2$  can be temperature dependent through internal voltage  $V_b$ . This can lead to slight increase of  $C_2$  with lowering temperature. And at low temperatures we enter into regime described by Fig. 4b. Thus,  $T_{CO}$  anomaly can be again interpreted as interplay of bulk and contact capacitance. As can be seen from 4-contacts resistance curve of sample S3 in Fig. 1, bulk resistance of PCMO increases rapidly at  $T_{CO}$ . This rapidly influences the balance of resistances in Fig. 4b, resulting in decrease of overall capacitance.

The temperature dependence of dielectric constant in Ref.<sup>20</sup> generally agrees with those presented here. The most visible difference is much stronger anomaly at  $T = T_{CO}$  in Ref.<sup>20</sup>. We interpret this by different contact material (GaIn paint) that was used in that study. Since contacts depend on type of metal used, it should be expected that contact capacitances have different temper-

ature dependence and also different breakdown voltages. Usage of rather high voltage of  $V=1V$  in this study could additionally influence Schottky capacitances.

Our measurements, in accordance with some reports<sup>25</sup>, suggest strongly that all reports of apparently colossal dielectric constant should pass detailed analysis in order to eliminate the possibility of Schottky barrier capacitances as the origin of anomalously large dielectric constant. As for the family of PCMO manganites, we hope that we proved such an origin. Our finding is emphasized by apparently colossal dielectric constant in other manganites ( $\text{CuCa}_3\text{Mn}_2\text{Ti}_2\text{O}_{12}$ ) that, contrary to PCMO, lack charge ordering or structural inhomogeneities.

### Acknowledgments

We acknowledge financial support from Ministerio de Educación y Ciencia (MAT2003-01880) and Comunidad de Madrid (07N/0080/2002). We thank S. Tomić and T. Vuletić for valuable discussions.

---

<sup>\*</sup> Electronic address: biskup@icmm.csic.es

<sup>1</sup> M.A. Subramanian, D. Li, N. Duan, B.A. Reisner and A.W. Sleight, *J. SolidStateChem.* **151**, 323 (2000).

<sup>2</sup> M.H. Cohen, J.B. Neaton, L.X. He, D. Vanderbilt, *Jour. Appl. Phys.* **94**, 3299 (2003); L.X. He, J.B. Neaton, M.H. Cohen, D. Vanderbilt, C.C. Homes, *Phys. Rev. B* **65**, 214112 (2002).

<sup>3</sup> P.Lunkenheimer, R.Fichtl, S.G.Ebbinghaus and A.Loidl, *Phys. Rev. B* **70**, 172102 (2004).

<sup>4</sup> For the review of this subject see E.Dagotto, T.Hotta and A.Moreo, *Physics Report* **344**, 1 (2001) or M.Ziese, *Rep. Prog. Phys.* **65**, 143 (2002).

<sup>5</sup> M.Uehara, S.Mori, C.H.Chen, S.-W.Cheong, *Nature* **399**, 560 (1999).

<sup>6</sup> M.Fäth, S.Freisem, A.A.Menovsky, Y.Yamioka, J.Aarts and J.A.Mydosh, *Science* **285**, 1540 (1999).

<sup>7</sup> Y.Tomioka, A.Asamitsu, H.Kuwahara, Y.Moritomo and Y.Tokura, *Phys. Rev. B* **53**, R1689 (1996).

<sup>8</sup> Z.Jirak, S.Krupicka, Z.Simsa, M.Dlouha, Z.Vratislav, *J. Magn. Magn. Mater.* **53**, 153 (1985).

<sup>9</sup> H.Yoshizawa, H.Kawano, Y.Tomioka and Y.Tokura, *Phys. Rev. B* **52**, R13145 (1995).

<sup>10</sup> A.Asamitsu, Y.Tomioka, H.Kuwahara and Y.Tokura, *Nature* **388**, 50 (1997).

<sup>11</sup> Y.Moritomo, A.Asamitsu, H.Kuwahara and Y.Tokura, *Phys. Rev. B* **55**, 7549 (1997).

<sup>12</sup> V.Kiryukhin, D.Casa, J.P.Hill, B.Keimer, A.Vigilante, Y.Tomioka and Y.Tokura, *Nature* **386**, 813 (1997).

<sup>13</sup> J. Sichelschmidt, M. Paraskevopoulos, T. Brando, R. Wehn, D. Ivannikov, F. Mayr, K. Pucher, J. Hemmer, A. Pimenov, H.A.K. von Nidda, P. Lunkenheimer, V.Y. Ivanov, A.A. Mukhin, A.M. Balbashov, A. Loidl, *Eur. Phys. J. B* **20**, 7 (2001).

<sup>14</sup> A.Anane, J.P.Renard, L.Reversat, C.Dupas, P.Veillet, M.Viret, L.Pinsard and A.Revcolevschi, *Phys. Rev. B* **59**, 77 (1999).

<sup>15</sup> S. Katano, J.A. Fernandez-Baca, Y. Yamada, *Physica B* **276-278**, 786 (2000).

<sup>16</sup> P.G. Radaelli, R.M. Ibberson, D.N. Argyriou, H. Casalta, K.H. Andersen, S.W. Cheong and J.F. Mitchell, *Phys. Rev. B* **63**, 172419 (2001).

<sup>17</sup> R. Kajimoto, T. Kakeshita, Y. Ohara, H. Yoshizawa, Y. Tomioka, Y. Tokura, *Phys. Rev. B* **58**, R11837 (1998).

<sup>18</sup> J.Tao and J.M.Zuo, *Phys. Rev. B* **69**, 180404 (2004).

<sup>19</sup> E.Dagotto, cond-mat/0302550v1 (2003).

<sup>20</sup> S.Mercone, A.Wahl, A.Pautrat, M.Pollet, C.Simon: *Phys. Rev. B* **69**, 174433 (2004).

<sup>21</sup> "Electronic Processes in Non-crystalline Materials", Mott and Davis, Clarendon Press, Oxford (1971).

<sup>22</sup> "Dielectric Relaxations in Solids", A.K.Jonscher, Chelsea Dielectric Press, London (1983).

<sup>23</sup> L.A.Dissado and R.M.Hill, *Phil. Mag. B* **41**, 625 (1980); L.A.Dissado and R.M.Hill, *J. Materials Science* **16**, 1410 (1981).

<sup>24</sup> Y.Tomioka, A.Asamitsu, Y.Moritomo and A.Tokura, *J. Phys. Soc. Jpn* **63**, 1689 (1995).

<sup>25</sup> P. Lunkenheimer, V. Bobnar, A.V. Pronin, A.I. Ritus, A.A. Volkov, A. Loidl, *Phys. Rev. B* **66**, 052105 (2002).